Atmos. Chem. Phys. Discuss., 8, 17739–17762, 2008
www.atmos-chem-phys-discuss.net/8/17739/2008/
© Author(s) 2008. This work is distributed under
the Creative Commons Attribution 3.0 License.

Atmospheric Chemistry and Physics Discussions

This discussion paper is/has been under review for the journal *Atmospheric Chemistry and Physics (ACP)*. Please refer to the corresponding final paper in *ACP* if available.

Severe ozone air pollution in the Persian Gulf region

J. Lelieveld[1,2], P. Hoor[2], P. Jöckel[1], A. Pozzer[1,2], P. Hadjinicolaou[1], and J.-P. Cammas[3]

[1]Energy, Environment and Water Research Centre, The Cyprus Institute, Nicosia, Cyprus
[2]MPI for Chemistry (Otto Hahn Institute), Mainz, Germany
[3]Observatoire Midi-Pyrénées, CNRS – Laboratoire d'Aérologie, Toulouse, France

Received: 8 August 2008 – Accepted: 16 August 2008 – Published: 29 September 2008

Correspondence to: J. Lelieveld (j.lelieveld@cyi.ac.cy)

Published by Copernicus Publications on behalf of the European Geosciences Union.

Abstract

Recently it was discovered that over the Middle East during summer ozone mixing ratios can reach a pronounced maximum in the middle troposphere. Here we extend the analysis to the surface and show that especially in the Persian Gulf region conditions are highly favorable for ozone air pollution. Model results indicate that the region is a hot spot of photo-smog where air quality standards are violated throughout the year. Long-distance transports of air pollution from Europe, the Middle East, natural emissions and stratospheric ozone conspire to bring about high background ozone mixing ratios. This provides a hotbed to indigenous air pollution in the dry local weather conditions, which are likely to get worse in future.

1 Introduction

Ozone (O_3) plays a key role in atmospheric oxidation processes and photochemical air pollution. Although there is no consensus about the critical levels for human health, environment agencies concur that 8-hourly levels in excess of 50–60 ppbv and a 1-hourly average of ~80 ppbv constitute health hazards (Ayres et al., 2006). Whereas high peak values are of particular importance for human health, permanent exposure to lower levels is also problematical (Bell et al., 2006). Furthermore, ambient mixing ratios of about 40 ppbv for extended periods of several months cause crop loss and damage to natural ecosystems (Emberson et al., 2003).

Ozone is a secondary pollutant, formed during the oxidation of reactive carbon compounds and catalyzed by nitrogen oxides (NO_x=NO+NO_2), driven by ultraviolet sunlight. Conditions typically found in the subtropics are conducive for the formation of photochemical smog, and background O_3 levels over the subtropical Atlantic have been observed to increase strongly by ~5 ppbv/decade (Lelieveld et al., 2004). In the Mediterranean region the European Union phytotoxicity limit of 40 ppbv and the health protection limit of 55 ppbv are often exceeded (Kouvarakis et al., 2002; Ribas

ACPD

8, 17739–17762, 2008

and Peñuelas, 2004), which causes tens of thousands of premature mortalities per year (Gryparis et al., 2004; Duncan et al., 2008).

In a study of vertical ozone profiles in the Middle East Li et al. (2001) used a global chemistry-transport model and predicted a regional summertime O_3 maximum in the middle troposphere in excess of 80 ppbv. Satellite measurements of tropospheric NO_2 confirm that O_3 precursor concentrations can be high in this area, also showing a strong positive trend in the last decade (van der A, 2008; Stavrakou et al., 2008). Li et al. (2001) concluded that transport from the stratosphere does not contribute significantly to the O_3 maximum. Yet, a study of stratosphere-troposphere exchange (STE) over the eastern Mediterranean indicates that cross-tropopopause transport can be intense, related to the distinct summertime meteorological conditions over South Asia and the Arabian Peninsula (Traub and Lelieveld, 2003).

Here we advance these investigations by applying the EMAC chemistry-general circulation model that represents STE processes as well as the large-scale transport and chemistry of air pollution (Roeckner et al., 2006; Jöckel et al., 2006). Our focus is on the Persian Gulf region, located downwind of major pollution areas and with substantial and growing local sources. It should be noted that this region is also subject to aerosol pollution, including desert dust (Fig. 1), though here we concentrate on ozone and the meteorological conditions that promote photochemical air pollution.

2 EMAC model description

The numerical model simulations have been performed with the 5th generation European Centre-Hamburg general circulation model, ECHAM5 (Roeckner et al., 2006) coupled to the Modular Earth Submodel System, MESSy (Jöckel et al., 2006), applied to Atmospheric Chemistry (EMAC). The model includes a comprehensive representation of tropospheric and stratospheric dynamical, cloud, radiation, multiphase chemistry and emission-deposition processes. We applied the model at T42 resolution, being about 2.8° in latitude and longitude. The vertical grid structure resolves the

ACPD
8, 17739–17762, 2008

lower and middle atmosphere with 90 layers from the surface to a top layer centered at 0.01 hPa (Giorgetta et al., 2006). This model configuration was selected because it explicitly represents stratosphere-troposphere interactions and includes a comprehensive representation of atmospheric chemistry, and also because it has been extensively tested and documented.

The chemistry calculations are performed using a kinetic preprocessor to describe a set of 177 gas phase, 57 photo-dissociation and 81 heterogeneous tropospheric and stratospheric reactions (Sander et al., 2005). Details of the chemical mechanism (including reaction rate coefficients and references) can be found in the electronic supplement. The model also carries a tracer for stratospheric ozone (O_3s), which enables a comparison with O_3 that is photochemically formed within the troposphere (Jöckel et al., 2006).

For the representation of natural and anthropogenic emissions and dry deposition of trace species, including micrometeorological and atmosphere-biosphere interactions, wet deposition by different types of precipitation, and multiphase chemistry processes we refer to the detailed descriptions by Ganzeveld et al. (2006), Kerkweg et al. (2006), Tost et al. (2006) and additional articles in a special issue of Atmospheric Chemistry and Physics. The results of the tropospheric and stratospheric chemistry calculations, using a number of diagnostic model routines, have been compared to in situ and remote sensing measurements (Jöckel et al., 2006; Lelieveld et al., 2007; Pozzer et al., 2007).

The model has been nudged towards actual meteorological conditions for the year 2006 based on operational analyses of the European Centre for Medium-range Weather Forecasts (ECMWF). A Newtonian relaxation term has been added to the prognostic variables for vorticity, divergence, temperature and surface pressure (Lelieveld et al., 2007). We avoid inconsistencies between the ECHAM5 and the ECMWF boundary layer representations by leaving the lowest three model levels free (apart from surface pressure), while the nudging increases stepwise in four levels up to about 700 hPa and tapers off to zero at 200 hPa.

Whilst the model has been extensively tested in many applications, an ozone mea-

ACPD
8, 17739–17762, 2008

surement database for the Middle East is to a large degree lacking. For the free troposphere we use ozone measurements of the MOZAIC program (Measurements of Ozone and Water Vapor by In-service Airbus Aircraft) (Thouret et al., 1998; Zbinden et al., 2006) (see also http://www.aero.obs-mip.fr/mozaic/). It appears that for 2000 and 2004 datasets are available from aircraft ascents and descents over Bahrain, Dubai, Kuwait and Riyadh, and we compared the measurements with model output for these years (Jöckel et al., 2006). Figure 2 shows that the pronounced middle tropospheric O_3 maximum in summer, which was predicted by Li et al. (2001), is reproduced.

For the year 2006 we use the 0.5 degree resolution satellite measurements of tropospheric ozone by the Tropospheric Emission Spectrometer (TES) (Worden et al., 2007; Osterman et al., 2008). Figure 3 compares these data to our model results along the satellite orbit, representative for three levels in the troposphere between 908.5 and 261 hPa over the Persian Gulf region. The individual TES data points produce a similar variability as the EMAC model results. Considering the difference in resolution and because the model nudging to ECMWF analyses approximates though not mimics meteorological conditions ideal agreement cannot be expected. From the agreement between the mean mixing ratios and the probability density functions we conclude that the model adequately represents atmospheric chemistry conditions in the Gulf region.

3 Meteorology

The large-scale Hadley circulation, driven by deep tropical cumulonimbus cloud formation and intense precipitation, induces descent in the subtropics. The low level circulation in the subtropics is characterized by vast anticyclones, which occupy about 40% of the Earth's surface (Rodwell and Hoskins, 2001). At the eastern flank of the Azores High the dry anticyclonic descent in summer extends over the Mediterranean, carrying European air pollutants southward to North Africa and the Middle East (Kallos et al., 1998; Lelieveld et al., 2002; Stohl et al., 2002; Duncan et al., 2004).

The Middle East, being under the downward branch of the Hadley circulation, is

ACPD
8, 17739–17762, 2008

among the warmest and driest in the world. From a space perspective, the atmospheric radiation budget is negative, i.e. the region radiates more infrared radiation than it receives sunlight (Vardavas, 2007). The net radiative cooling to space is balanced by entrainment of high-energy air in the upper troposphere while low-energy air is detrained near the surface. Mass conservation requires descent, which leads to the evaporation of clouds and suppression of rain. Since the tropics are expanding under the influence of global change (Seidel et al., 2008), it is expected that subsidence and dryness in the region will increase, which is considered a robust prediction of climate models (Giorgi and Bi, 2005; Held and Soden, 2006; Diffenbaugh et al., 2007; Sun et al., 2007).

In summer the hot desert conditions give rise to a heat low with cyclonic flow over the southern Arabian Peninsula. In the south the circulation is reinforced by the summer monsoon that carries air from East Africa. Over the Persian Gulf it converges with the northwesterly flow from the Mediterranean. In winter the Atlantic westerlies carry relatively clean air masses over the Mediterranean towards the Gulf. From the autumn to spring winds over the Gulf are more variable than in summer, nevertheless often carrying air masses southward, e.g. from Iran. Occasionally, storms carry desert dust plumes over the region, though during the wet season in winter the levels of dust and air pollution are reduced.

In summer the Asian monsoon surface trough and the Arabian heat low are associated with anticyclones in the upper troposphere. The tropical easterly jet stream at the southern flank of the monsoonal anticyclone is diverted toward the eastern Mediterranean by the Arabian anticyclone (Barret et al., 2008). Convergence of this flow with the polar front jet stream accelerates the horizontal wind and increases the horizontal and vertical wind shear, creating a jet streak and deep tropopause folds (Traub and Lelieveld, 2003). These carry ozone from the stratosphere and descend over the eastern Mediterranean and the Middle East.

4 Regional ozone hot spot

Figure 4a shows the daily and annual profiles of O_3 near the surface over the Persian Gulf, averaged over a region of 5° latitude and 10° longitude, i.e. an area of about 0.5 million km^2. Figure 4a also shows the contribution by ozone transported from the stratosphere (O_3s). It thus appears that most of the O_3 is formed photochemically within the troposphere, although the contribution by O_3s is non-negligible. In winter the mean diel O_3 variation is about 10–15 ppbv, related to photochemical O_3 formation during daytime and O_3 titration by NO emissions and dry deposition in the nocturnal boundary layer. In summer the diel variation is 20–30 ppbv owing to the rapid formation during daytime.

The annual O_3 minimum occurs in late December when the intensity of sunlight is lowest, whereas the contribution by STE is largest (~30%). The regional O_3 levels are highest in summer, on average about 75 ppbv, while daytime values often exceed 80 ppbv. Note that these high mixing ratios occur throughout the Gulf region, providing a hotbed for local smog formation near cities and industrial areas. Importantly, the diel mean O_3 mixing ratios substantially exceed 40 ppbv throughout the year, hence the EU air quality standard for phytotoxicity is permanently violated. Furthermore, the EU health protection limit is strongly exceeded between February and October.

The average global distribution of O_3 mixing ratios during summer is shown in Fig. 5 and the regional monthly means in Fig. 6, further illustrating that the Gulf region is a hot spot of notoriously high ozone. Note that we use a color scale from 40–80 ppbv and upward to emphasize where air quality standards are violated. The mean wind vectors near the surface indicate that the Gulf is downwind of air pollution sources in the Mediterranean region and the Middle East, including the megacities Cairo and Teheran.

Figure 4b presents the regional mixing ratios of carbon monoxide (CO), being an indicator of air pollution. The CO levels are generally high, comparable to industrialized environments in Europe. The synoptic variability of O_3 follows that of CO, i.e. on

ACPD
8, 17739–17762, 2008

time scales of days to weeks, which underscores that the ozone is to a large degree produced in polluted air.

Figure 4c shows peroxyacetylnitrate (PAN), a noxious pollutant formed from hydrocarbons and NO_x. The synoptic variability of PAN correlates with both CO and O_3, whereas its seasonality anticorrelates with O_3. PAN is decomposed thermally so that in summer its lifetime is short. On the other hand, PAN builds up in winter, illustrated by the steep increase in November and December. Because of its increasing lifetime with decreasing temperature, PAN can act as a reservoir species of NO_x (Singh et al., 1998). It is formed during transport from polluted regions upwind and thermally decomposes over the warm Gulf region where it adds to ambient NO_x levels.

The transport characteristics of ozone and precursor gases give rise to year round high O_3 mixing ratios over the Gulf. Our model results suggest that in the entire region from Riyadh to Dubai, during all seasons, a distinct O_3 maximum is located between the surface and ~750 hPa (Fig. 7). Clearly the Gulf is a convergence region of long-distance transported air pollution, which fosters strong local O_3 formation by indigenous emissions of NO_x and reactive hydrocarbons, e.g. from oil and petrochemical industries and urban areas. The regional O_3 maximum is most pronounced in summer when the meteorological conditions are auspicious for photo-smog.

Although the contribution by STE to surface ozone may seem limited it is interesting to examine its role throughout the tropospheric column. Previously, Li et al. (2001) investigated the middle tropospheric O_3 maximum over the Middle East in summer. At variance with Li et al. our model results point to a significant role of STE (Fig. 7). Nevertheless, we agree with Li et al. that also in the middle and upper troposphere in situ photochemical O_3 formation plays an important role, and the anthropogenic component substantially contributes to the radiative forcing of climate.

In fact, STE derived ozone penetrates remarkably far south over the Middle East. Especially in winter and spring an O_3s maximum reaches deeply into the tropics in the lower free troposphere. Interestingly, a second O_3s maximum touches the surface near the Gulf around 30° N latitude, both in summer and winter. This corresponds to

ACPD
8, 17739–17762, 2008

the results in Fig. 4a, showing that the contribution of O_3s is significant during the entire year.

Figure 8 presents a global and longitudinal cross section of O_3s during summer, averaged between 25–30° N latitude. The influence of deep convection in the South Asian monsoon region, around 90° E (near the Mt. Everest), is apparent from the relatively low O_3s mixing ratios throughout the troposphere. To the west, between about 500 and 600 hPa, two O_3s maxima appear, resulting from deep tropopause folding events. In particular the one near 30° E represents unusually deep subtropical STE. Figure 8 illustrates that a tongue of O_3s reaches the surface over the Persian Gulf, unique in the subtropics.

5 Comparison with other locations

A combination of factors thus contributes to the ozone maximum over the Gulf. To put this into perspective we compare with other subtropical locations in both hemispheres.

Since our global model is not ideal for investigating local urban and industrial conditions, we selected locations that are representative of larger areas. The largest city in the world in terms of surface area is Los Angeles, also notorious for high ozone levels. Although the Los Angeles emissions of CO per capita are among the highest in the world, its emission normalized per surface area is lowest of the 20 largest cities (Gurjar et al., 2008). This is indicative of a relatively widespread and uniform source distribution.

For our comparison we define a "greater Los Angeles area" with a size close to a single grid cell in our model, also encompassing some ocean area and surrounding cities such as Pasadena, Riverside and San Bernardino. Similarly, we define a "greater Bahrain area", which includes a fraction of the Gulf, part of Qatar and several coastal cities in Saudi Arabia.

Figure 9 presents a comparison between these two polluted areas and also to more rural locations in southern China (Hunan), western Australia, and an area over the

ACPD
8, 17739–17762, 2008

subtropical Pacific near Midway, downwind of China. None of these regions is free of anthropogenic influence while the level of O_3 decreases from the top down. Figure 9 shows that all of these subtropical locations, irrespective of their remoteness, have O_3 mixing ratios close to or in excess of the EU air quality standard for phytotoxicity. This underscores the sensitivity of the subtropical latitude belt to anthropogenic emissions.

The vicinity of these five locations to pollution sources is illustrated by the amplitude of the diel O_3 cycle. In Los Angeles the local emissions are strongest, leading to a rapid photochemical O_3 build-up during the day and nighttime O_3 titration by NO emissions. In Bahrain the diel amplitude is smaller because the ambient O_3 levels are more strongly determined by long-distance transport. In Hunan and W-Australia the diel O_3 amplitude is increasingly smaller at greater distance from strong NO_x sources.

In marine environments such as Midway, with negligible local NO_x sources, the diel O_3 cycle is controlled by upwind photochemical destruction during daytime and the absence of photochemistry at night (de Laat and Lelieveld, 2000). The remoteness from NO_x sources is also illustrated by the seasonal cycle of O_3. In polluted environments the season with the most intense sunlight is associated with the strongest O_3 production, whereas in remote low-NO_x locations photochemical O_3 loss prevails. Usually in summer the influence of STE becomes negligible (Fig. 9). However, this is not the case in the Gulf region.

Surprisingly, during summer the daily mean O_3 mixing ratios in Bahrain are similar to Los Angeles although daytime peak levels can be higher in the latter. In winter Los Angeles is subject to westerly winds that carry unpolluted Pacific air. Conversely, in Bahrain during winter O_3 levels are substantially higher, i.e. permanently in excess of 40 ppbv.

Figure 9 also shows model calculated O_3 levels after excluding anthropogenic sources (in green). Generally, the diel and annual profiles much resemble clean maritime conditions and most locations have O_3 mixing ratios of about 20 ppbv or less. Only in Bahrain during summer ozone levels approach 40 ppbv, indicating substantial influence from upwind natural NO_x emissions, especially lightning (Li et al., 2001).

ACPD
8, 17739–17762, 2008

6 Conclusions

The ozone hot spot over the Persian Gulf predicted by our model calculations is caused by a combination of factors that operate in the same direction. These include long-distance transport of air pollution, unusually strong STE, substantial upwind natural NO_x sources, a lack of deep convective mixing and precipitation, local emissions and favorable conditions for photochemistry. Together this leads to high ozone mixing ratios both in the free troposphere and the boundary layer.

Although here we focus on 2006 it is important to emphasize that the ozone hot spot over the Persian Gulf is a recurrent feature in our model calculations for the period 1996–2006. Furthermore, a model run for the summer of 2006 at T106 resolution (~1.1° lat/lon) reproduces the ozone hot spot, indicating that the results presented here are not an artifact of the model resolution.

Our model has been extensively tested for many locations and we consider these results compelling. Further, data from satellites and upwind subtropical regions indicate increasing trends of ozone and precursors. Nevertheless, the lack of ground-based measurements in the Gulf region is unsatisfactory. We recommend that Global Atmospheric Watch stations in Saudi Arabia and Iran report the available data and that additional stations are set up to provide the information needed to effectively reduce air pollution. This will be particularly important as it may be expected that climate change will promote poor air quality conditions while O_3 precursor emissions will continue to increase in the region.

Acknowledgements. We are grateful to V. Thouret, the MOZAIC (Measurements of Ozone and Water Vapor by In-service Airbus Aircraft) and TES teams (Tropospheric Emission Spectrometer on NASA's Aura satellite) for the use of data to test our model. We acknowledge the support of MOZAIC by the European Commission, Airbus and INSU-CNRS. Particular thanks to Lufthansa, Air France and Austrian Air for carrying the MOZAIC equipment free of charge since 1994.

The publication of this article is financed by the Max Planck Society.

References

Ayres, J., Maynard, R., and Richards, R.: Air pollution and health, Imperial College Press, London, UK, 248 pp., 2006.

Barret, B., Ricaud, P., Mari, C., Attié, J.-L., Bousserez, N., Josse, B., Le Flochmoën, E., Livesey, N. J., Massart, S., Peuch, V.-H., Piacentini, A., Sauvage, B., Thouret, V., and Cammas, J.-P.: Transport pathways of CO in the African upper troposphere during the monsoon season: a study based upon the assimilation of spaceborne observations, Atmos. Chem. Phys., 8, 3231–3246, 2008, http://www.atmos-chem-phys.net/8/3231/2008/.

Bell, M. L., Peng, R. D., and Dominici, F.: The exposure-response curve for ozone and risk of mortality and the adequacy of current ozone regulations, Environ. Health Perspect., 114, 532–536, 2006.

de Laat, A. T. J. and Lelieveld, J.: Diurnal ozone cycle in the marine boundary layer, J. Geophys. Res., 105, 11 547–11 559, 2000.

Diffenbaugh, N. S., Pal, J. S., Giorgi, F., and Gao, X.: Heat stress intensification in the Mediterranean climate change hotspot, Geophys. Res. Lett., 34, L11706, doi:10.1029/2007GL030000, 2007.

Duncan, B. N. and Bey, I.: A modeling study of the export pathways of pollution from Europe: Seasonal and interannual variations (1987–1997), J. Geophys. Res., 109, D08301, doi:10.1029/2003JD004079, 2004.

Duncan, B. N., West, J. J., Fiore, A. M., and Ziemke, J. R.: The influence of European pollution on ozone in the Near East and northern Africa, Atmos. Chem. Phys., 8, 2267–2283, 2008, http://www.atmos-chem-phys.net/8/2267/2008/.

Emberson, L., Ashmore, M., and Murray, F.: Air pollution impacts on crops and forests: a global assessment, Imperial College Press, London, UK, 372 pp., 2003.

Ganzeveld, L. N., van Aardenne, J. A., Butler, T. M., Lawrence, M. G., Metzger, S. M., Stier,

P., Zimmermann, P., and Lelieveld, J.: Technical Note: Anthropogenic and natural offline emissions and the online EMissions and dry DEPosition submodel EMDEP of the Modular Earth Submodel system (MESSy), Atmos. Chem. Phys. Discuss., 6, 5457–5483, 2006, http://www.atmos-chem-phys-discuss.net/6/5457/2006/.

Giorgetta, M. A., Manzini, E., Roeckner, E., Esch, M., and Bengtsson, L.: Climatology and forcing of the quasi-biennial oscillation in the MAECHAM5 model, J. Climate, 19, 3882–3901, 2006.

Giorgi, F. and Bi, X.: Updated regional precipitation and temperature changes for the 21st century from ensembles of recent AOGCM simulations, Geophys. Res. Lett., 32, L21715, doi:10.1029/2005GL024288, 2005.

Gryparis, A., Forsberg, B., Katsouyanni, K., et al.: Acute effects of ozone on mortality from the "Air pollution and health: a European approach" project, Am. J. Respir. Crit. Care Med., 170, 1080–1087, 2004.

Gurjar, B. R., Butler, T. M., Lawrence, M. G., and Lelieveld, J.: Evaluation of emissions and air quality in megacities, Atmos. Environ., 42, 1593–1606, 2008.

Held, I. M. and Soden, B. J.: Robust responses of the hydrological cycle to global warming, J. Climate, 19, 5686–5699, 2006.

Jöckel, P., Tost, H., Pozzer, A., Brühl, C., Buchholz, J., Ganzeveld, L., Hoor, P., Kerkweg, A., Lawrence, M. G., Sander, R., Steil, B., Stiller, G., Tanarhte, M., Taraborelli, D., van Aardenne, J., and Lelieveld, J.: The atmospheric chemistry general circulation model ECHAM5/MESSy: Consistent simulation of ozone from the surface to the mesosphere, Atmos. Chem. Phys., 6, 5067–5104, 2006, http://www.atmos-chem-phys.net/6/5067/2006/.

Kerkweg, A., Sander, R., Tost, H., and Jöckel, P.: Technical Note: Implementation of prescribed (OFFLEM), calculated (ONLEM), and pseudo-emissions (TNUDGE) of chemical species in the Modular Earth Submodel System (MESSy), Atmos. Chem. Phys., 6, 3603–3609, 2006, http://www.atmos-chem-phys.net/6/3603/2006/.

Kallos, G., Kotroni, V., Lagouvardos, K., and Papadopoulos, A.: On the long-range transport of air pollutants from Europe to Africa, Geophys. Res. Lett., 25, 619–622, 1998.

Kouvarakis, G., Vrekoussis, M., Mihalopoulos, N., Kourtidis, K., Rappenglueck, B., Gerasopoulos, E., and Zerefos, C.: Spatial and temporal variability of tropospheric ozone (O_3) in the boundary layer above the Aegean Sea (eastern Mediterranean), J. Geophys. Res., 107, 8137, doi:10.1029/2000JD000081, 2002.

Lelieveld, J., Berresheim, H., Borrmann, S., et al.: Global air pollution crossroads over the

Mediterranean, Science, 298, 794–799, 2002.
Lelieveld, J., van Aardenne, J., Fischer, H., de Reus, M., Williams, J., and Winkler, P.: Increasing ozone over the Atlantic Ocean, Science, 304, 1483–1487, 2004.
Lelieveld, J., Brühl, C., Jöckel, P., Steil, B., Crutzen, P. J., Fischer, H., Giorgetta, M. A., Hoor, P., Lawrence, M. G., Sausen, R., and Tost, H.: Stratospheric dryness: model simulations and satellite observations, Atmos. Chem. Phys., 7, 1313–1332, 2007, http://www.atmos-chem-phys.net/7/1313/2007/.
Li., Q., Jacob, D. J., Logan, J. A., Bey, I., Yantosca, R. M., Liu, H., Martin, R. V., Fiore, A. M., Field, B. D., and Duncan, B. N.: A tropospheric ozone maximum over the Middle East, Geophys. Res. Lett., 28, 3235–3238, 2001.
Osterman, G. B., Kulawik, S. S., Worden, H. M., Richards, N. A. D., Fisher, B. M., Eldering, A., Shephard, M. W., Froidevaux, L., Labow, G., Luo, M., Herman, R. L., Bowman, K. W., and Thompson, A. M.: Validation of Tropospheric Emission Spectrometer (TES) measurements of the total, stratospheric, and tropospheric column abundance of ozone, J. Geophys. Res., 113, D15S16, doi:10.1029/2007JD008801, 2008
Pozzer, A., Jckel, P., Tost, H., Sander, R., Ganzeveld, L., Kerkweg, A., and Lelieveld, J.: Simulating organic species with the global atmospheric chemistry general circulation model ECHAM5/MESSy1: a comparison of model results with observations, Atmos. Chem. Phys., 7, 2527–2550, 2007, http://www.atmos-chem-phys.net/7/2527/2007/.
Roeckner, E., Brokopf, R., Esch, M., Giorgetta, M., Hagemann, S., Kornblüh, L., Manzini, L. E., Schlese, U., and Schulzweida, U.: Sensitivity of simulated climate to horizontal and vertical resolution in the ECHAM5 atmosphere model, J. Climate, 19, 3771–3791, 2006.
Rodwell, M. J. and Hoskins, B. J.: Subtropical anticyclones and the summer monsoon, J. Climate, 14, 3192–3211, 2001.
Sander, R., Kerkweg, A., Jöckel, P., and Lelieveld, J.: Technical note: The new comprehensive atmospheric chemistry module MECCA, Atmos. Chem. Phys., 5, 445–450, 2005, http://www.atmos-chem-phys.net/5/445/2005/.
Seidel, D. J., Fu, Q., Randel, W. J., and Reichler, T. J.: Widening of the tropical belt in a changing climate, Nature Geosc., 1, 21–24, 2008.
Singh, H. B., Chen, Y., Thakur, A. N., Kondo, Y., Talbot, R. W., Gregory, G. L., Sachse, G. W., Blake, D. R., Bradshaw, J. D., Wang, Y., and Jacob, D. J.: Latitudinal distribution of reactive nitrogen in the free troposphere over the Pacific Ocean in late winter/early spring, J. Geophys. Res., 103, 28 237–28 246, 1998.

ACPD
8, 17739–17762, 2008

Stohl, A., Eckhardt, S., Forster, C., James, P., and Spichtinger, N.: On the pathways and timescales of intercontinental air pollution transport, J. Geophys. Res., 107, 4684, doi:10.1029/2001JD001396, 2002.

Stavrakou, T., Müller, J.-F., Boersma, K. F., De Smedt, I., and van der A, R. J.: Assessing the distribution and growth rates of NO_x emission sources by inverting a 10-year recors of NO_2 columns, Geophys. Res. Lett., 35, L10801, doi: 10.1029/2008GL033521, 2008.

Sun, Y., Solomon, S., Dai, A., and Portmann, R. W.: How often will it rain?, J. Climate, 20, 4801–4818, 2007.

Thouret, V., Marenco, A., Logan, J. A., Nédélec, P., and Grouhel, C.: Comparisons of ozone measurements from the MOZAIC airborne program and the ozone sounding network at eight locations, J. Geophys. Res., 103, 695–720, 1998.

Tost, H., Jöckel, P., Kerkweg, A., Sander, R., and Lelieveld, J.: Technical note: A new comprehensive SCAVenging submodel for global atmospheric chemistry modelling, Atmos. Chem. Phys., 6, 565–574, 2006, http://www.atmos-chem-phys.net/6/565/2006/.

Traub., M. and Lelieveld, J.: Cross-tropopause transport over the eastern Mediterranean, J. Geophs. Res., 108, 4712, doi:10.1029/2003JD003745, 2003.

van der A, R. J., Eskes, H. J., Boersma, K. F., van Noije, T. P. C., van Roozendaal, M., de Smedt, I., Peters, D. H. M. U., and Meijer, E. W.: Trends, seasonal variability and dominant NO_x sources derived from a ten year recors of NO_2 measured from space, J. Geophys. Res., 113, D04302, doi:10.1029/2007JD009021, 2008.

Vardavas, I. M. and Taylor, F. W.: Radiation and climate, Oxford University Press, Oxford, 512 pp., UK, 2007.

Worden, H. M., Logan, J. A., Worden, J. R., Beer, R., Bowman, K., Clough, S. A., Eldering A., Fischer, B. M., Gunson, M. R., Herman, R. L., Kulawik, S. S., Lampel, M. C., Luo, M., Megretskaia, I. A., Osterman, G. B., and Shephard, M. W.: Comparisons of Tropospheric Emission Spectrometer (TES) ozone profiles to ozonesondes: Methods and initial results, J. Geophys. Res., 112, D03309, doi:10.1029/2006JD007258, 2007.

Zbinden, R. M., Cammas, J.-P., Thouret, V., Nèdèlec, P., Karcher, F., and Simon, P.: Mid-latitude tropospheric ozone columns from the MOZAIC program: climatology and interannual variability, Atmos. Chem. Phys., 6, 1053–1073, 2006, http://www.atmos-chem-phys.net/6/1053/2006/.

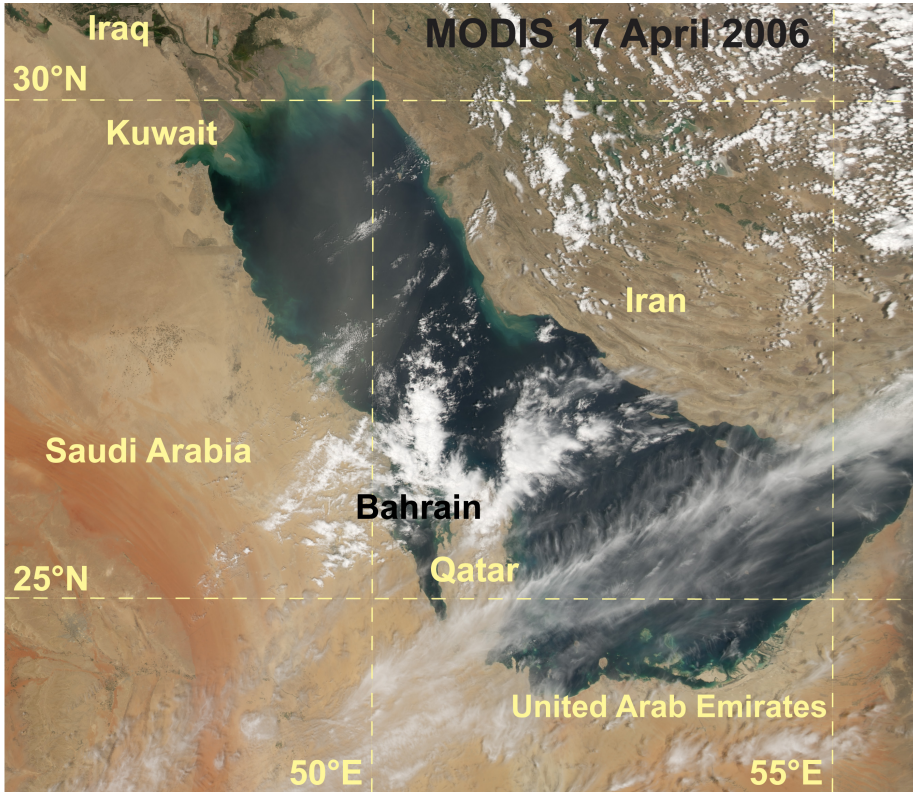

Fig. 1. Satellite image of the Persian Gulf region by the Moderate resolution Imaging Spectrometer taken on 17 April 2006, showing thin clouds and desert dust transported from the west (NASA Visible Earth).

ACPD
8, 17739–17762, 2008

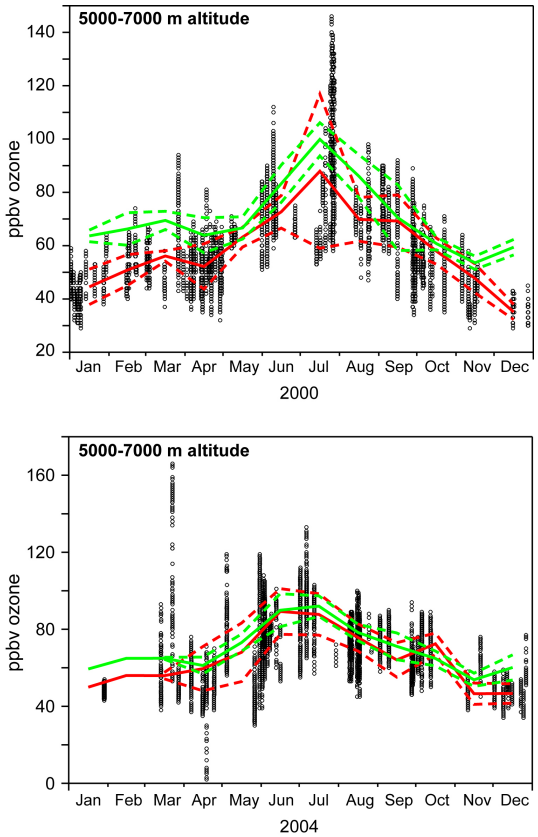

Fig. 2. Compilation of MOZAIC aircraft measurements over Bahrain, Dubai, Kuwait and Riyadh compared to model calculated O_3 in the middle troposphere over the Middle East. The black circles indicate the individual measurement data points, the red solid lines the monthly mean measured O_3, the solid green lines the monthly mean modeled O_3 mixing ratios and the dashed lines the monthly standard deviations.

ACPD
8, 17739–17762, 2008

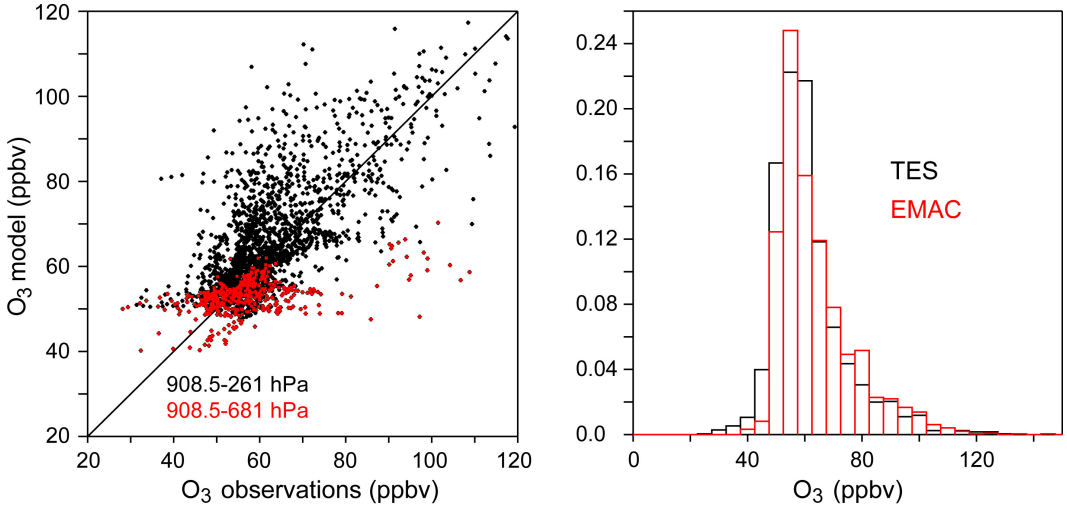

Fig. 3. Compilation of TES satellite observations compared to EMAC model calculated O_3 in the troposphere in the region of 25–30° N and 45–55° E latitude in the year 2006. Left: correlation plot in which the solid line indicates ideal agreement. The red symbols highlight the O_3 mixing ratios at the lowest altitude level resolved by TES. Right: probability density functions.

ACPD
8, 17739–17762, 2008

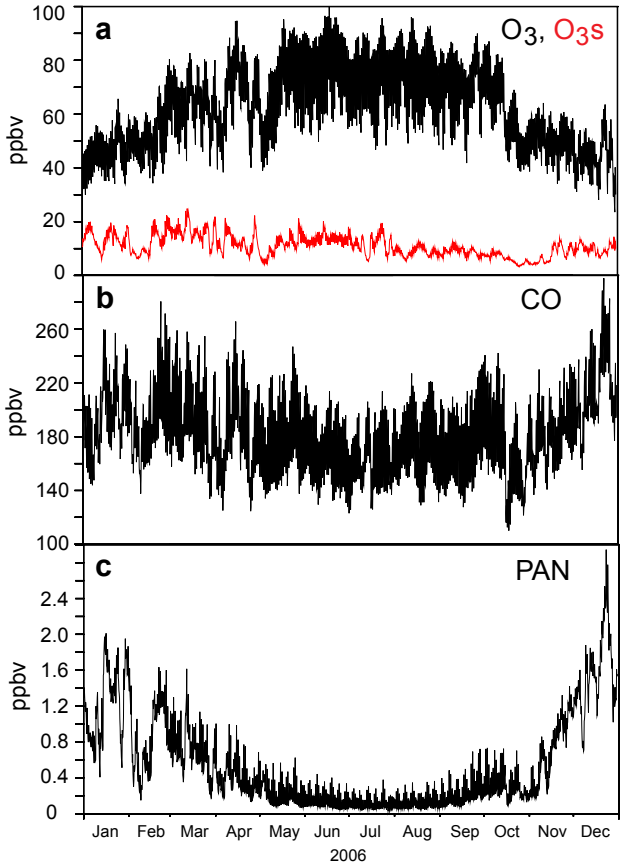

Fig. 4. Model calculated ozone, CO and PAN near the surface in the region of 25–30° N and 45–55° E. In red the contribution by ozone transported from the stratosphere (O_3s).

ACPD
8, 17739–17762, 2008

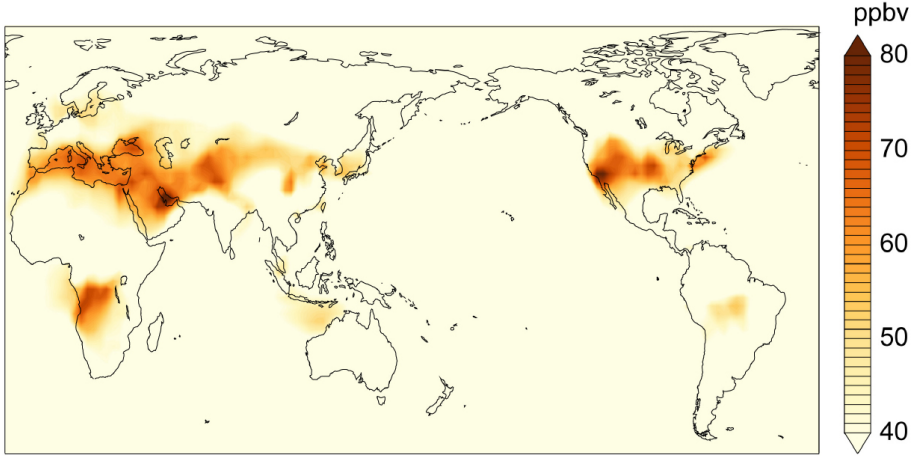

Fig. 5. Model calculated mean surface ozone in excess of 40 ppbv averaged over the period July-August 2006, highlighting the subtropical band of ozone smog and pronounced hot spots over the Los Angeles and Persian Gulf regions.

ACPD
8, 17739–17762, 2008

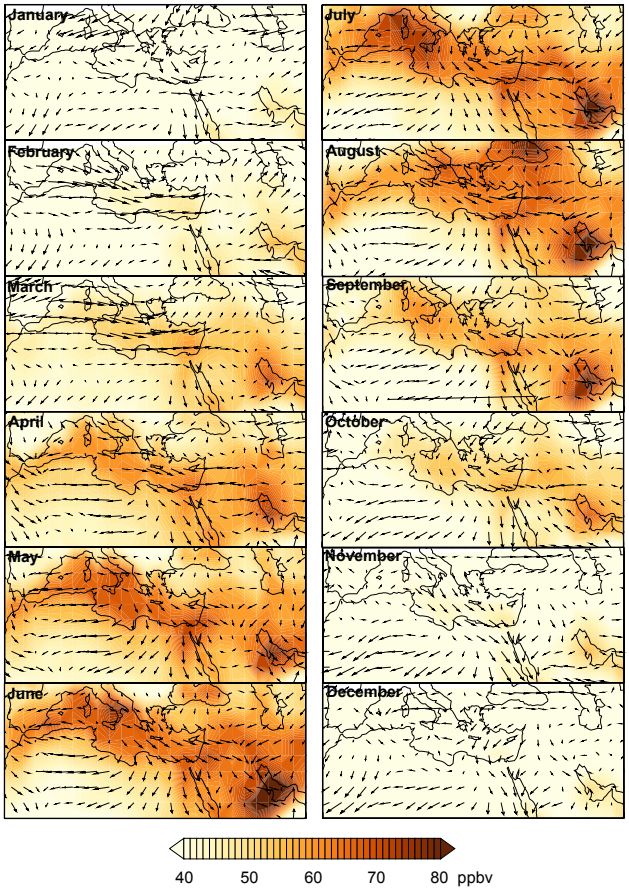

Fig. 6. Model calculated monthly mean surface ozone in excess of 40 ppbv in the period January to December 2006. The arrows indicate the mean surface winds.

ACPD
8, 17739–17762, 2008

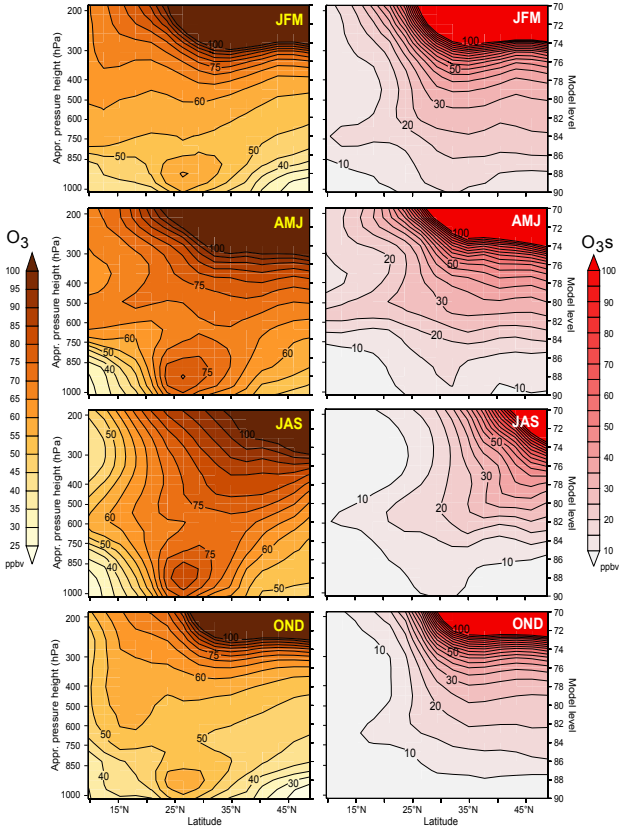

Fig. 7. Model calculated 3-monthly mean zonal and vertical distribution of O_3 (left) and O_3 originating in the stratosphere (O_3s, right) averaged over the 45–55° E longitude belt.

ACPD
8, 17739–17762, 2008

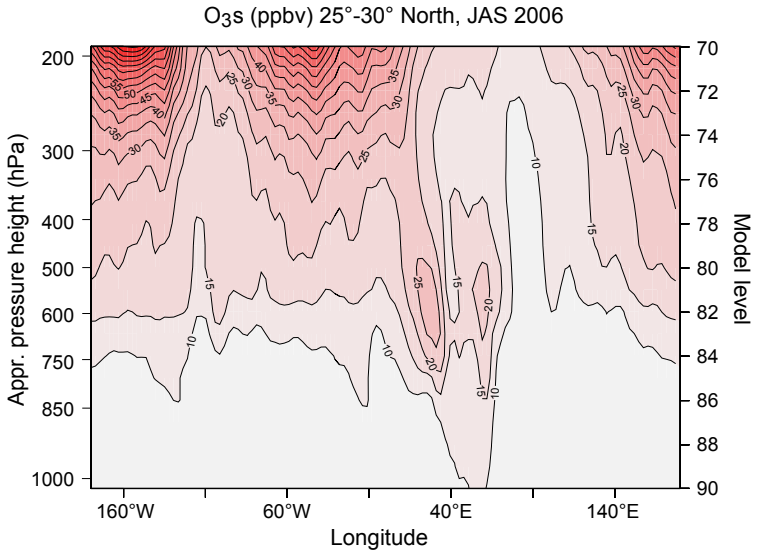

Fig. 8. Model calculated tropospheric ozone originating in the stratosphere (O_3s) averaged between 25–30° N latitude in the period July to September 2006.

ACPD
8, 17739–17762, 2008

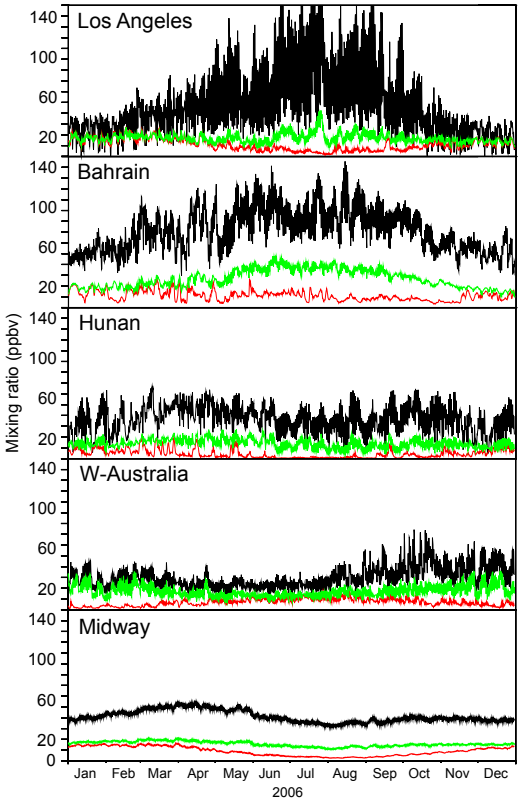

Fig. 9. Model calculated surface mixing ratios of ozone and O_3s (red) in the areas of Los Angeles (117–119° W, 33–35° N), Bahrain (50–52° E, 25–27° N), Hunan in China (109–110° E, 26–28° N), West Australia (118–120° E, 26–28° S) and the Pacific Midway Islands (180° E–178° W, 26–28° N). The green curves show ozone with a model setup in which anthropogenic emissions were excluded.

ACPD
8, 17739–17762, 2008